Theoret. chim. Acta (Berl.) 23, 115—126 (1971)

Commentationes

Ab Initio versus CNDO Barrier Calculations

I. N_2H_4 and N_2F_4

E. L. WAGNER

Department of Chemistry, Washington State University, Pullman, Washington 99163, USA

Received April 29, 1971

Ab initio SCF-LCAO-MO calculations of the barriers to internal rotation have been performed for N_2H_4 and N_2F_4 using a small basis of gaussian functions. A single rotamer is predicted for N_2H_4 at 94° with *cis* and *trans* barriers of 9.64 and 3.67 kcal/mole. For N_2F_4 there are two stable forms (64° and 180°), the *trans* configuration being more stable by 1.5 kcal/mole. The computed barrier separating *gauche* from *trans* N_2F_4 is 5.7 kcal/mole. CNDO and INDO barrier curves agree qualitatively but not quantitatively. The barrier curves are best reflected by the sums of all overlap populations across the N–N bonds.

Für die Moleküle N_2H_4 und N_2F_4 wurden *ab initio* SCF-LCAO-MO-Berechnungen der Barrieren der inneren Rotation mit einer kleinen Basis von Gaussfunktionen durchgeführt. Für N_2H_4 wird ein einziges Rotameres bei 94° mit *cis*- und *trans*-Barrieren von 9,64 und 3,67 kcal/mol berechnet. Beim N_2F_4 gibt es zwei stabile Formen (64° und 180°), wobei die *trans*-Konfiguration um 1,5 kcal/mol stabiler ist. Die berechnete Barriere zwischen *gauche*- und *trans*-Form be N_2F_4 beträgt 5,7 kcal/mol. Die nach den beiden Methoden CNDO und INDO bestimmten Kurven stimmen qualitativ, aber nicht quantitativ überein. Der Verlauf der Barrierenkurven wird am besten durch die Summe aller Überlappungspopulation der N–N-Bindungen widergespiegelt.

Calculs *ab-initio* SCF LCAO MO des barrières de rotation interne pour N_2H_4 et N_2F_4 en utilisant une petite base de fonctions gaussiénnes. On prévoit l'existence d'un rotamère unique pour N_2H_4 à 94° avec des barrières *cis* et *trans* de 9,64 et 3,67 kcal/mole. Pour N_2F_4 il y a deux formes stables (64° et 180°), la configuration *trans* étant favorisée par 1,5 kcal/mole. La barrière calculée entre les formes *gauche* et *trans* de N_2F_4 est 5,7 kcal/mole. L'accord est qualitatif mais non quantitatif avec les courbes donnant la barrière dans les méthodes CNDO et INDO. Les courbes de barrière sont mieux représentées par les sommes de toutes les populations de recouvrement à travers la liaison N–N.

Introduction

In recent years a number of *ab initio* all-electron self-consistent-field type calculations have been carried out on simple molecules in the hope of elucidating the nature of the barriers to internal rotation. These calculations apparently give reasonable values for the magnitudes of the barriers, and they seem to agree well with the experimentally deduced stable configurations of the gaseous compounds.

Unfortunately, these calculations are very extravagant with computer time so attempts have been made to estimate barrier heights for internal rotation and

Table 1. *Geometrical parameters used for* N_2H_4 *and* N_2F_4

Parameter	N_2H_4	N_2F_4
N–N distance	1.499 Å	1.53 Å
N–X distance	1.022 Å	1.393 Å
XNX angle	106°	103.7°
NNX angle	112°	101.3°

to predict the stable configurations using semiempirical methods of calculation. We here compare our *ab initio* calculations on hydrazine (N_2H_4), and tetrafluorohydrazine (N_2F_4) with the corresponding calculations on the same molecules using the semiempirical CNDO and INDO methods of Pople *et al.* [1–3].

Only in the case of hydrazine have *ab initio* type calculations previously been reported [4–6], and we have used these results to appraise the adequacy of our method of calculation. Microwave studies on hydrazine [7, 8], although incomplete, do confirm the theoretical predictions that only the *gauche* rotamer with a dihedral angle near 90° is stable. From this study the experimental barrier height was estimated to be 3.14 ± 0.15 kcal/mole when the unlikely assumption was made that the *cis* and *trans* barriers were equal.

In the case of tetrafluorohydrazine, N_2F_4, it appears that both the *gauche* and *trans* forms, with dihedral angles of 60–70° and 180°, respectively, exist in equilibrium with each other and have approximately the same energies [9–12]. The two forms are apparently separated by a barrier of 4–7 kcal/mole [13]. In our calculations on N_2F_4 we used the averaged geometry obtained from electron diffraction studies [14], although more recent work gives somewhat shorter NN and NF distances [12].

The values for all of the geometrical parameters used in the computations are shown in Table 1. In our calculations, as is the custom, we varied only the dihedral angles in going from one point to another although there are undoubtedly deformations in other parameters as the dihedral angle is changed and these may well have significant effects on the energies [15].

Methods of Calculation

The *ab initio* method used here for the calculation of the molecular wave functions and the molecular energies is the conventional Hartree-Fock-Roothaan SCF-LCAO-MO method in which all integrals are evaluated analytically [16]. The actual computations were carried out using the computer program IBMOL [17], which computes the wave functions of molecular systems using gaussian orbitals. All of the calculations were performed on the IBM System 360 Model 67 computer of the Washington State University Computing Center.

Our canonical gaussian orbital basis set used three *s*-type gaussians centered on each hydrogen atom, and seven *s*-type plus nine *p*-type (three in each direction) on each nitrogen and fluorine atoms. Thus, for N_2H_4 we used 44 gaussian orbitals whose orbital exponents were optimized for the separated atoms and then not

Table 2. *Orbital exponents of the gaussian functions for hydrogen, nitrogen, and fluorine*

	Hydrogen	Nitrogen	Fluorine
		s-type functions	
1	4.500370	636.101	1448.6612
2	0.681277	105.386	122.282223
3	0.151374	27.5167	55.219578
4		9.02708	17.303336
5		3.33086	6.312729
6		0.828625	1.3769414
7		0.243109	0.40502026
		p-type functions	
8		5.19829	8.9238
9		1.10716	1.84090
10		0.26175	0.40607

Table 3. *Contracted gaussian sets for hydrogen, nitrogen, and fluorine*[a]

1*s*(H):	$0.070480\,\chi_1 + 0.407890\,\chi_2 + 0.647669\,\chi_3$
1*s*(N):	$0.018231\,\chi_1 + 0.108122\,\chi_2 + 0.324286\,\chi_3 + 0.478333\,\chi_4 + 0.221201\,\chi_5$
2*s*(N):	$0.466703\,\chi_6 + 0.596283\,\chi_7$
2*p*(N):	$0.138430\,\chi_8 + 0.497601\,\chi_9 + 0.575051\,\chi_{10}$
1*s*(F):	$0.012709\,\chi_1 + 0.085081\,\chi_2 + 0.290095\,\chi_3 + 0.482837\,\chi_4 + 0.261361\,\chi_5$
2*s*(F):	$0.508534\,\chi_6 + 0.555137\,\chi_7$
2*p*(F):	$0.154710\,\chi_8 + 0.520809\,\chi_9 + 0.554338\,\chi_{10}$

[a] The $\chi_1, \chi_2, \ldots$ are the gaussian functions whose exponents are given in Table 2.

varied any further. This molecular basis of 44 gaussian orbitals was then 'contracted' to 14 orbital functions corresponding to the various 1*s*, 2*s*, and 2*p* atomic orbitals in the N_2H_4 molecule [18]. For N_2F_4, we used 96 basis gaussian orbitals for the whole molecule contracted to 30 orbital functions representing the 1*s*, 2*s*, $2p_x$, $2p_y$, and $2p_z$ atomic orbitals on each of the six atoms in the molecule. The orbital exponents and the contraction coefficients used for the different atoms are given in Tables 2 and 3 [19].

In the semiempirical CNDO and INDO calculations we used the computer program CNINDO [20]. These methods consider only the valence-shell electrons which are all treated explicitly. Overlap integrals are neglected and the other one-electron integrals are calculated empirically. The zero differential overlap approximation is adopted for the electron repulsion integrals and the remaining two-electron integrals are replaced by averaged values. In spite of this imbalance between one- and two-electron terms, these particular semiempirical methods should be more satisfactory than the strictly one-electron semiempirical methods, such as the extended Hückel procedure.

Results

N_2H_4. In Table 4 the calculated barriers to internal rotation for hydrazine are summarized, and in Fig. 1 our total calculated energies are plotted as functions of the dihedral angles. The dihedral angle is taken to be the angle between the bisectors of the two HNH angles, the *cis* (eclipsed) configuration corresponding to a dihedral angle of 0°.

Our small-sized basis set *ab initio* calculation correctly gives the proper stable configurations and predicts barrier magnitudes in fair agreement with those of the more extensive calculations (Table 4). The contention that the barrier curve is relatively insensitive to the size of the basis set [21] again seems to be substanti-

Table 4. *Calculated barriers to internal rotation in hydrazine (kcal/mole)*

	Veillard [4]	Pedersen and Morokuma [5]	Fink, Pan and Allen [6]	This work			Expt'l
				ab initio	CNDO	INDO	
cis-barrier	11.5	11.05	11.88	9.64	1.74	2.08	(3.14) [8]
trans-barrier	4.7	6.21	3.70	3.67	2.23	3.19	
stable form	94°	~90°	~100°	94°	65°	70°	~90°

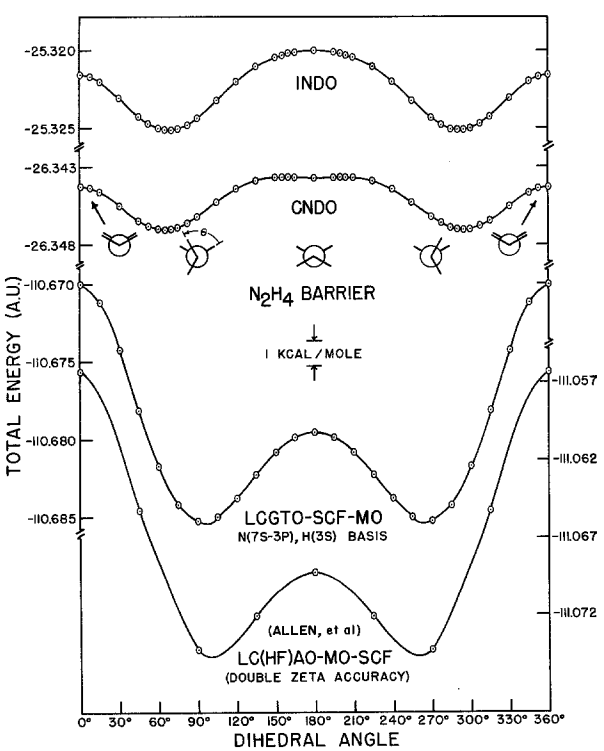

Fig. 1. Calculated energy barrier curves for N_2H_4

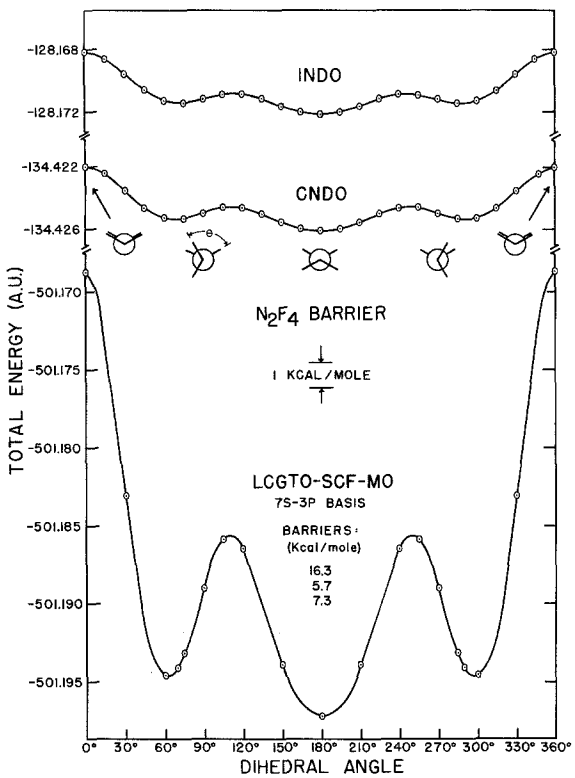

Fig. 2. Calculated energy barrier curves for N_2F_4

Table 5. *Calculated barriers to internal rotation in tetrafluorohydrazine (kcal/mole)*

	ab initio	CNDO	INDO	Experimental [12, 13]
cis-barrier	16.3	2.125	2.015	
gauche-barrier	5.7	0.502	0.377	4–7
trans-barrier	7.3	0.985	0.86	
stable forms	64°, 180°	68°, 180°	69°, 180°	67°, 180°

ated. The semiempirical CNDO and INDO results both qualitatively reflect the results of the more sophisticated calculations in that they correctly predict only stable *gauche* configurations, but the calculated dihedral angles of 65° and 70°, respectively, are certainly significantly different from the value of 94° of the extended calculations and of experiment. Furthermore, these semiempirical methods here greatly underestimate the magnitude of the *cis* barrier in comparison with the *ab initio* calculations.

N_2F_4. The results of the energy calculations on tetrafluorohydrazine are shown in Fig. 2 and Table 5. From the *ab initio* results we predict that both the

Table 6. *Calculated* SCF *energies for* N_2H_4 *and* N_2F_4

Dihedral Angle	N_2H_4				N_2F_4			
	Total energy	V_{nn}	V_{ee}	$T+V_{ne}$	Total energy	V_{nn}	V_{ee}	$T+V_{ne}$
0°	−110.67004	41.223790	79.103450	−230.99728	−501.16876	280.45346	473.47841	−1255.1006
15°	−110.67121	41.221699	79.100523	−230.99343				
30°	−110.67427	41.215967	79.094012	−230.98424	−501.18310	278.91347	471.88171	−1251.9783
45°	−110.67815	41.207946	79.088850	−230.97495	−501.19134	277.49418	470.43613	−1249.1216
60°	−110.68713	41.199185	79.089265	−230.97018	−501.19466	276.11026	469.06225	−1246.3672
65°					−501.19463	275.68885	468.65304	−1245.5365
70°					−501.19411	275.29047	468.27047	−1244.7551
75°	−110.68420	41.190846	79.097013	−230.97206	−501.19317	274.91097	467.90976	−1244.0139
90°	−110.68526	41.183443	79.111566	−230.98026	−501.18898	273.84511	466.90706	−1241.9411
105°	−110.68499	41.176932	79.130889	−230.99281	−501.18584	272.75986	465.87323	−1239.8189
120°	−110.68381	41.171057	79.152046	−231.00692	−501.18646	271.56332	464.69642	−1237.4462
135°	−110.68227	41.165740	79.171745	−231.01975				
150°	−110.68084	41.161276	79.187156	−231.02928	−501.19391	269.22086	462.31082	−1232.7256
165°	−110.67988	41.158232	79.196663	−231.03478				
180°	−110.67955	41.157145	79.199831	−231.03652	−501.19722	268.20335	461.25579	−1230.6564

gauche and *trans* forms of N_2F_4 are stable, with the *trans* configuration more stable by about 1.5 kcal/mole. These calculations predict the *cis* barrier to be very high, 16.3 kcal/mole; the other two barriers are in agreement with the experimental prediction [13], being 5.7 and 7.3 kcal/mole, respectively, from the *gauche* and *trans* positions. The *gauche* dihedral angle calculates to be about 64°, again in agreement with the experimental expectation. The calculated energy terms for N_2F_4 and N_2H_4 as functions of the dihedral angles are given in Table 6. The semiempirical calculations on N_2F_4 again reflect the *ab initio* results, correctly predicting the proper stable configurations, but once more greatly underestimating the magnitudes of the barriers. These methods, however, do correctly vaticinate the *trans* form to be the more stable configuration.

Discussion

The energy barrier curves of N_2H_4 and N_2F_4, as shown in Figs. 1 and 2, differ qualitatively from one another in that N_2H_4 has an energy barrier for the *trans* position while N_2F_4 exhibits an energy minimum. It appears that N_2F_4 has the more expected behavior and that N_2H_4 may then represent the egregious case. The origins of these kinds of rotational barriers have previously been considered from several points of view using the results of *ab initio* calculations. Analysis of the barrier mechanism from an energy standpoint has often been utilized. The nuclear-nuclear potential repulsion energies do not reflect the barrier curves for either N_2H_4 or N_2F_4. However, the attractive ($V_{att} = V_{ne}$) and repulsive ($V_{rep} = V_{nn} + V_{ee} + T$) energy components, into which the total energy may be partioned, seem to show opposing phase relations as functions of the dihedral angles thus showing a delicate balance of forces which changes as the molecules rotate [21]. This is shown for N_2H_4 and N_2F_4 in Fig. 3. For hydrazine, these curves have been interpreted as indicating that both the *cis* and *trans* barriers are 'repulsive dominant' because the V_{rep} terms, in going from 0° to 94° and from 180° to 94°, decrease faster than the V_{att} components increase [21]. Thus, in the mutually competing interactions of the various rotating electrons and nuclei, the repulsive terms apparently dominate as both the *cis* and *trans* barriers in hydrazine are approached. On the other hand, in N_2F_4, while the *cis* barrier from 0° to 64° and the first *gauche* barrier from 112° to 64° are again both repulsive dominant, the second *gauche* barrier from 180° to 112° appears to be attractive dominant. However, the magnitudes of these component energy changes for N_2F_4 are nearly 100 times larger than those for N_2H_4, even though the absolute differences in these terms are about the same in both molecules.

In certain cases the trends of the gross atomic and overlap populations seem to correlate with the barrier curves [22, 23]. Fig. 4 shows the total atomic populations of the atoms in N_2H_4 and N_2F_4 as functions of the dihedral angles. These data were obtained from the Mulliken population analyses [24] of the SCF wavefunctions from our *ab initio* calculations. In the case of N_2H_4, it is seen that as the molecule is rotated from the *cis* toward the *trans* configuration, charge is transferred monotonically to the nitrogen atoms from the bonded hydrogen atoms; this charge goes to the N-atom *p*-orbitals perpendicular to the N–N

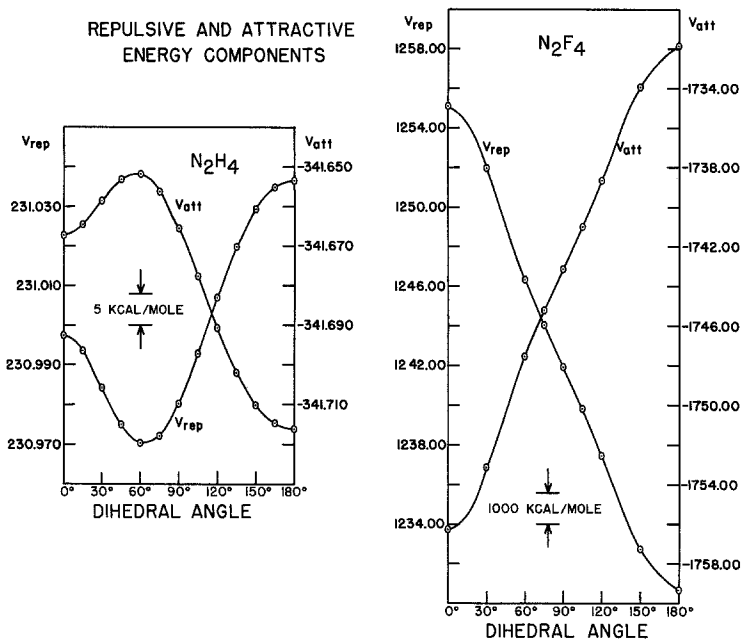

Fig. 3. Attractive and repulsive energy components *versus* dihedral angles for N_2H_4 and N_2F_4

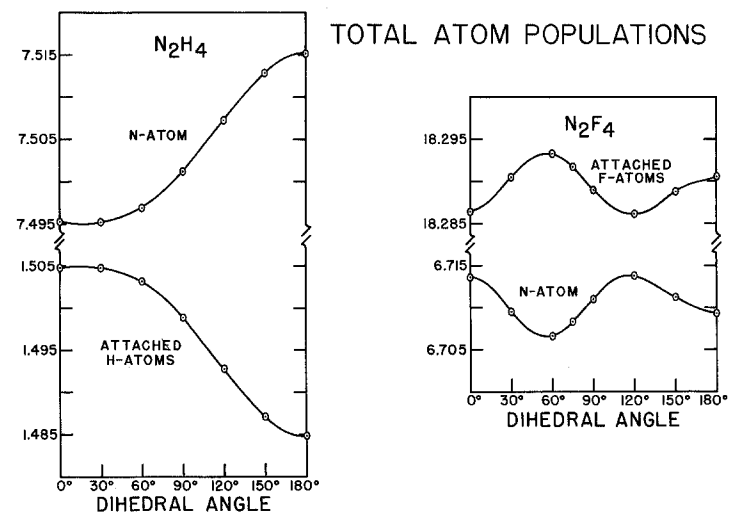

Fig. 4. SCF gross atomic populations as functions of the dihedral angles for N_2H_4 and N_2F_4

bond axis. Here the charge variations do not reflect the barrier curve. However, in the case of N_2F_4, the charge first flows off of the nitrogen atoms onto the attached fluorine atoms, then back onto the nitrogen atoms, and finally back again to the fluorine atoms; thus the maxima of charge on the nitrogen atoms do reflect the

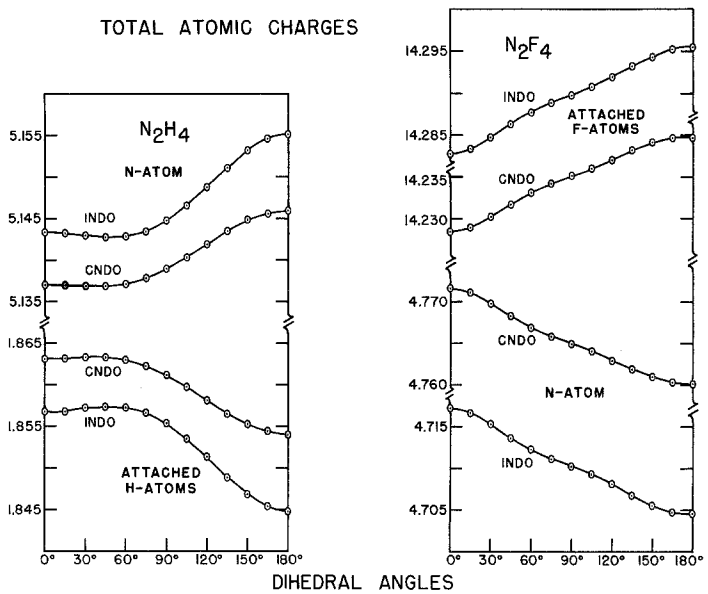

Fig. 5. CNDO and INDO total atomic charges as functions of the dihedral angles for N_2H_4 and N_2F_4

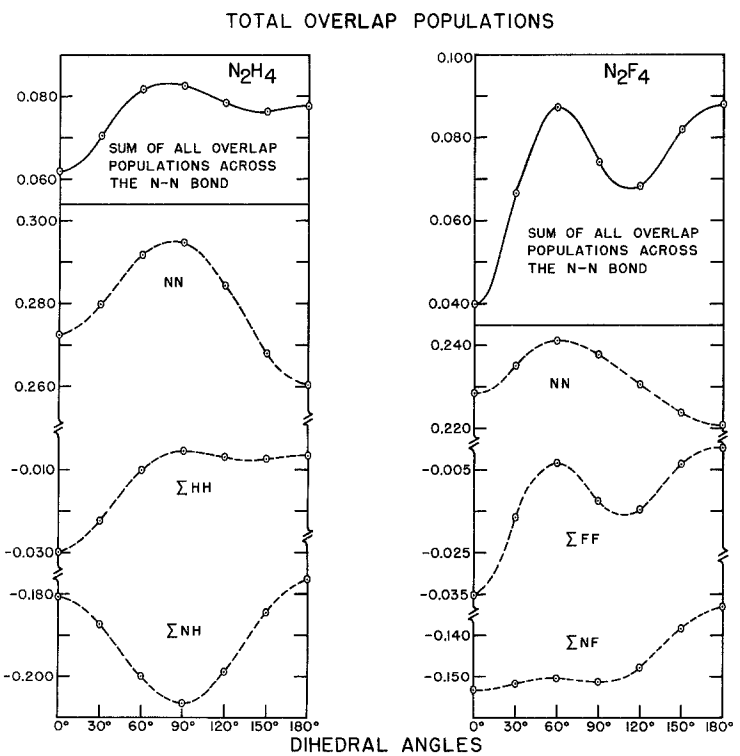

Fig. 6. SCF total overlap populations as functions of the dihedral angles for N_2H_4 and N_2F_4

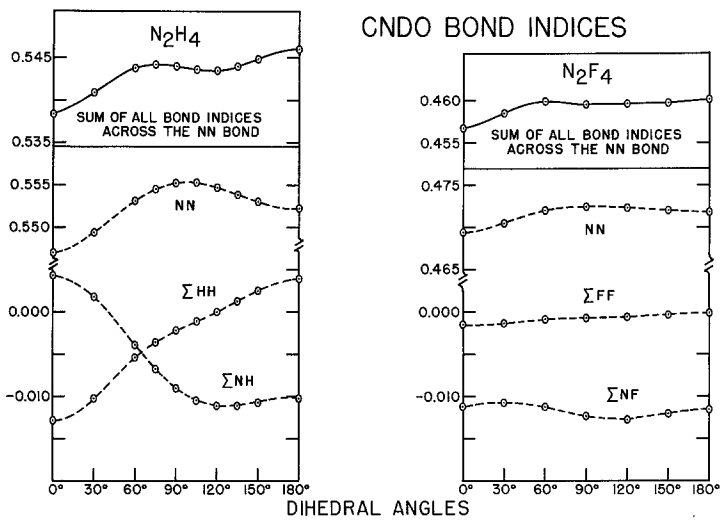

Fig. 7. CNDO total bond indices as functions of the dihedral angles for N_2H_4 and N_2F_4

barriers. These charge redistributions do not occur in such a way that the nuclear shieldings minimize the FF′ and HH′ interactions in the eclipsed configurations.

The variations of atomic charge for N_2H_4 and N_2F_4 as calculated by the semiempirical CNDO methods are shown in Fig. 5. The curves for N_2H_4 show trends similar to those from the *ab initio* treatment and still do not reflect the barrier curve. The curves for N_2F_4 are not in agreement with the corresponding charge variations from the *ab initio* calculations, nor do they now reflect the calculated barrier curve. In addition, the trends in the semiempirical N_2F_4 atomic charges are opposite to those of N_2H_4 in that the nitrogen atoms now monotonically lose charge to the attached fluorine atoms as the dihedral angle increase toward 180°.

The overlap populations between the atoms across the N–N bond in N_2H_4 and N_2F_4 as functions of the dihedral angles calculated from the SCF wavefunctions are shown in Fig. 6. For both molecules there are maxima in the NN bond orders near the stable *gauche* configurations, but not at the stable *trans* configuration for N_2F_4. In the case of N_2H_4, the sum of all the overlap populations across the NN bond fairly well reflects the barrier curve, although all of the factors (NN′, NH′, and HH′ overlap populations) individually contribute to the overall effect and have maxima or minima near the stable *gauche* configuration. In the case of N_2F_4, the sum of all the overlap populations across the NN bond again reflects the barrier curve, showing maximum total bond orders at the stable configurations. This curve, and therefore the barrier curve for N_2F_4, is characterized primarily by the FF′ interactions. The agreement here is better than in the N_2H_4 case, perhaps indicating that the lone-pair interactions are less important for N_2F_4 than for N_2H_4.

The CNDO and INDO 'Bond Indices' [25], $P_{AB} = \sum_{\mu}^{A} \sum_{\nu}^{B} P_{\mu\nu} S_{\mu\nu}$, are shown as functions of the dihedral angles in Fig. 7. For N_2H_4, none of the bond index

curves reflect the energy barrier curve calculated by the CNDO and INDO methods. For N_2F_4, the sum of all the bond indices more nearly reflects the barrier curve than do any of the individual components. However, these bond indices obtained from the semiempirical wavefunctions do not vary with the barriers as faithfully as do the total overlap populations from the *ab initio* wavefunctions.

Conclusions

The energy barrier curves for N_2H_4 and N_2F_4 generated by the *ab initio* SCF-LCGTO-MO method correctly predict the geometries of the stable configurations and give reasonable magnitudes for barriers to internal rotation which are in agreement with existing experimental predictions. Analysis of the SCF wavefunctions indicates that the qualitative distinction between the barrier curves of N_2H_4 and N_2F_4 results from the fact that the N_2F_4 barrier curve is characterized primarily by the change in the FF′ interactions with dihedral angle while in N_2H_4 the HH′, NH′, and NN′ interactions all vary with comparable magnitudes and have essentially equal influences in determining the overall barrier curve.

The barrier curves calculated by the semiempirical CNDO and INDO methods qualitatively reflect the *ab initio* curves in that they correctly predict the actual number of stable rotamers in each case, but they significantly underestimate the magnitudes of the barriers as well as generate fallacious values for the dihedral angles.

Acknowledgements. The author would like to acknowledge the generous assistance of Dr. David W. Klint with the computations and express his gratitude to the Washington State Computing Center for their generosity in providing computer time.

References

1. Pople, J. A., Santry, D. P., Segal, G. A.: J. chem. Physics **43**, S 129 (1965).
2. — Segal, G. A.: J. chem. Physics **43**, S 136 (1965); **44** 3289 (1966).
3. Pople, J. A., Beveridge, D. L., Dodosh, P. A.: J. chem. Physics **47**, 2026 (1967).
4. Veillard, A.: Theoret. chim. Acta (Berl.) **5**, 413 (1966).
5. Pedersen, L., Morokuma, K.: J. chem. Physics **46**, 3941 (1967).
6. Fink, W. H., Pan, D. C., Allen, L. C.: J. chem. Physics **47**, 895 (1967).
7. Kasuya, T.: Sci. Pap. Inst. physic. chem. Res. **56**, 1 (1962).
8. — Kojima, T.: J. physic. Soc. Japan **18**, 364 (1963).
9. Oskam, A., Elst, R., Duinker, J. C.: Spectrochim. Acta **26** A, 2021 (1970).
10. Durig, J. R., Clark, J. W.: J. chem. Physics **48**, 3216 (1968).
11. Koster, D. F., Miller, F. A.: Spectrochim. Acta **24** A, 1487 (1968).
12. Cardillo, M. J., Bauer, S. H.: Inorg. Chem. **8**, 2086 (1969).
13. Colburn, C. B., Johnson, F. A., Haney, C.: J. chem. Physics **43**, 4526 (1965).
14. Bohn, R. K., Bauer, S. H.: Inorg. Chem. **6**, 304 (1967).
15. Sovers, O. J., Karplus, M.: J. chem. Physics **44**, 3033 (1966).
16. Roothaan, C. C. J.: Rev. mod. Physics **23**, 69 (1951); **32**, 179 (1960).
17. Program obtained from E. Clementi, IBM Research Laboratory, San Jose, Calif.
18. Clementi, E., Davis, D. R.: J. comput. Physics **1**, 223 (1966).
19. — Andre, J., Andre, M., Klint, D., Hahn, D.: Acta Physica **27**, 493 (1969).
20. Dobosh, P. A.: Program No. 141, Quantum Chemistry Program Exchange, Chemistry Department, Indiana University, Bloomington, Indiana 47401, USA.

21. Allen, L. C.: Chem. Physics Letters **2**, 597 (1968).
22. Schwartz, M. E.: J. chem. Physics **51**, 4182 (1969).
23. — Hayes, E. F., Rothenberg, S.: J. chem. Physics **52**, 2011 (1970); Theoret. chim. Acta (Berl.) **19**, 98 (1970).
24. Mulliken, R. S.: J. chem. Physics **23**, 1833, 1841, 2338, 2343 (1955).
25. Ehrenson, S., Seltzer, S.: Theoret. chim. Acta (Berl.) **20**, 17 (1971).

Prof. Dr. E. L. Wagner
Department of Chemistry
Washington State University
Pullman, Washington 99163, USA